*Geomicrobiology Journal*, 22:283–298, 2005

ISSN: 0149-0451 print / 1362-3087 online
DOI: 10.1080/01490450500183654

Taylor & Francis
Taylor & Francis Group

# Carbonate Mineralogy Along a Biogeochemical Gradient in Recent Lacustrine Sediments of Gallocanta Lake (Spain)

**A. Corzo**
*Departamento de Biología, Facultad de Ciencias del Mar y Ambientales, Universidad de Cádiz, Polígono Río San Pedro, 11510-Puerto Real, Spain*

**A. Luzon and M. J. Mayayo**
*Departamento Ciencias de la Tierra. Universidad de. Zaragoza. Pedro Cerbuna, 12. 50009-Zaragoza, Spain*

**S. A. van Bergeijk**
*Departamento de Biología, Facultad de Ciencias del Mar y Ambientales, Universidad de Cádiz, Polígono Río San Pedro, 11510-Puerto Real, Spain*

**P. Mata**
*Departamento de Geología, Facultad de Ciencias del Mar y Ambientales, Universidad de Cádiz, Polígono Río San Pedro, 11510-Puerto Real, Spain*

**J. García de Lomas**
*Departamento de Biología, Facultad de Ciencias del Mar y Ambientales, Universidad de Cádiz, Polígono Río San Pedro, 11510-Puerto Real, Spain*

**Three sedimentary subenvironments, palustrine (GP), marginal lacustrine (GML) and central lacustrine (GCL), were compared regarding water chemistry and microbial activity in order to explain the differences in the carbonate mineralogical composition of the upper sediment layer in Gallocanta Lake, a shallow hypersaline environment in Northeastern Spain. Horizontal heterogeneity was considerable, salinity ranged from 5 to 116 (‰) for the GP and GCL subenvironments respectively. Sulfate, $Mg^{2+}$, and $Ca^{2+}$ concentrations covaried among them and with salinity. The relative abundance of Mg-bearing carbonates, including high-Mg calcite, dolomite and hydrated Ca-magnesite, increased with the salinity. They were absent from the GP subenvironment, where only calcite precipitates, and maximum abundances were found in the GCL subenvironment (61%), where salinity, sulfate, and $Mg^{2+}$ concentrations were highest. Every subenvironment presented specific microecological characteristics. The microbial community of the GCL subenvironment lacked of oxygenic photosynthesis, while the microbial communities of GML and GP subenvironments were photosynthetically active. Vertical profiles of sulfide and pH at the water-sediment interface revealed clear differences between the GCL and GML subenvironments as well. Sulfide was detected below the oxic layer in the GCL subenvironment and increased with depth, but it was undetected in the GML subenvironment. The precipitation of Mg-bearing carbonates with different Mg:Ca proportions occurs at different stage along a biogeochemical gradient, where increasing salinity and sulfate content favour the anaerobic oxidation of organic carbon by dissimilatory sulfate reduction.**

**Keywords** carbonate precipitation, dolomite, magnesite, microelectrodes, sulfate-reducing bacteria, geomicrobiology, bacterial dolomite model

Received 10 January 2005; accepted 3 May 2005.

This work has been supported by grants of the Spanish Ministry of Science and Technology no: REN-2000-1136-CLI, MAT-2000-0261-P4-04, REN-2002-01281 and by the E28 DGA project (Analysis of continental sedimentary basins). S. A. van Bergeijk was supported by a Marie Curie fellowship of the European Community programme "Improving Human Research Potential and the Socio-Economic Knowledge Base" under contract number HPMF-CT-2000-00994. Authors thank Dr. Y. van Lith, Prof. Dr. R. Reitner and two anonymous reviewers by their comments and suggestions.

Address correspondence to Alfonso Corzo, Departamento de Biología, Facultad de Ciencias del Mar y Ambientales, Polígono Río San Pedro, 11510-Puerto Real, Spain. E-mail: alfonso.corzo@uca.es

## INTRODUCTION

Dolomite is a calcium-magnesium carbonate ($CaMg(CO_3)_2$) with a variable distribution through the sedimentary record. Dolomite is common in ancient sedimentary rocks, but it is absent or very scarce in Holocene and recent sedimentary sequences (Warren 2000 and references therein). Attempts to precipitate dolomite under sterile conditions at low temperature have been unsuccessful even for very long incubation periods (Land 1998). These paradoxical facts are the basis of

the so-called "Dolomite Problem," which has been extensively discussed in the geological literature (Fairbridge 1957; Machel and Mountjoy 1986; Gunatilaka 1987; Last 1990; McKenzie 1991; Warren 2000).

Vasconcelos et al. (1995) reported the precipitation of dolomite in sediment samples from a coastal lagoon (Lagoa Vermelha, Brazil) incubated under anoxic conditions in the presence of sulfate-reducing bacteria (SRB). The so-called "microbial dolomite model" was formulated by Vasconcelos and McKenzie (1997) to account for the involvement of SRB in the primary precipitation of $Mg^{2+}$-bearing carbonates. This model has gained acceptance as more laboratory experiments (Warthmann et al. 2000; van Lith et al. 2003b) and field observation were conducted (Vasconcelos and McKenzie 1997; Wright 1999; van Lith et al. 2002, 2003b). The hypothesis of an implication of SRB in dolomite precipitation was not new (Nadson 1928; Neher 1959; Gunatilaka 1987; Middelburg et al. 1990), but had been largely neglected in the voluminous literature on the "Dolomite Problem," as pointed out by Vasconcelos and McKenzie (1997). In addition to dolomite, SRB mediate the precipitation of other types of carbonates with variable proportions of Ca and Mg in different environments (Jørgensen and Cohen 1977; Gunatilaka 1987; Pontoizeau et al. 1997; Visscher et al. 1998; Castanier et al. 2000; Dupraz et al. 2004).

Microbial-facilitated dolomite precipitation is reported to occur almost exclusively in saline-hypersaline environments like Arabian Gulf sabkhas (Gunatilaka 1987; Gunatilaka et al. 1987; Chafetz et al. 1999), the Coorong area of South Australia (Wright 1999), Lagoa Vermelha in Brazil (Vasconcelos and McKenzie 1997; van Lith et al. 2002) and in marine organic-rich deepwater sediments (Baker and Burns 1985; Compton and Siever 1986; Compton 1988; Middelburg et al. 1990). All these are coastal lagoons or marine environments and the main source of sulfate is seawater. The study of possible microbial-induced precipitation of dolomite in Gallocanta Lake is interesting in this context because: (1) There is evidence that dolomite and several other Ca-Mg carbonates could be precipitating there at present (Comín et al. 1990; Mayayo et al. 2003). (2) From a geological point of view this lake differs from environments where microbial-induced dolomite precipitation has been reported previously.

Gallocanta Lake is an endorheic water body, where the main source of sulfate is an important underground flow across saline and calcareous Mesozoic formations (Pérez et al. 2002). Moreover, Gallocanta Lake is ecologically very different from Lagoa Vermelha, which is probably the best-studied environment where microbial-induced dolomite precipitation has been reported. Lagoa Vermelha is a coastal lagoon and dolomite precipitation seems to occur within a black, anoxic organic-carbon-rich sludge on top of the sediment (Vasconcelos and McKenzie 1997; van Lith et al. 2002). Such a black sludge is absent from the water-sediment interface in Gallocanta Lake. The study of new sites where dolomite is precipitating at present is important to develop dolomite precipitation models and to interpret the genetic conditions of ancient dolomites.

The sediment surface in Gallocanta Lake is colonised by benthic microbial communities, usually dominated by cyanobacteria as the major photoautotrophic component. These communities may form microbial mats. Both the photosynthetic and heterotrophic microorganisms, including SRB, that inhabit these benthic microbial communities have been reported to be involved in the precipitation of various types of carbonate minerals (Jorgensen and Cohen 1977; Morita 1980; Thompson and Ferris 1990; Visscher et al. 1998; Castanier et al. 1999; Sagemann et al. 1999; Riding 2000; Dupraz et al. 2004). Processes of biomineralization taking place within these benthic microbial communities occur in a chemical microenvironment dominated by steep gradients of various organic and inorganic compounds. One of the major challenges of geomicrobiology is to better characterise the physico-chemical microenvironment where the microbial-induced precipitation process occurs. This microenvironment, as result of microbial metabolism, is generally very different from the bulk conditions in the water column or in the sediments (Schultze-Lam et al. 1996).

In this paper, we describe the chemical microenvironment of the water-sediment interface at three different sites at the Gallocanta Lake by means of $O_2$, $H_2S$, pH, and Eh microelectrodes. These sites represent different subenvironments within Gallocanta Lake characterised by the different sedimentary processes and facies, and by their different mineralogical paragenesis. Important differences among sites were found in the microbial community and its metabolic activity. We discuss how the differences in the composition of the microbial communities and their metabolic activities, together with differences in water chemistry, are related to the type of carbonates currently occurring at each of the sites.

## AREA DESCRIPTION

The Gallocanta Lake (40°59′N, 1°30′W; 990 m above sea level) is the largest saline wetland in the northeast of the Iberian Peninsula. It is a shallow (<2 m) hypersaline ephemeral lake situated in the central sector of the Iberian Range (Figure 1). The lake basin lies mainly over Triassic deposits (carbonates and evaporites) and it is bounded by Ordovician rocks (mainly quartzites) to the N-NE, and by Mesozoic carbonate rocks to the S-SW. Moreover, Quaternary coarse detritic sediments are common around the lake edges. Climate in the region is subarid Mediterranean with a high continental influence. The average temperature varies from −15°C in January to 29.5°C in July. The average annual rainfall is 448 mm, with maxima in autumn and spring. The mean annual potential evaporation is 926 mm. Because of the imbalance between precipitation and evaporation, the water volume changes considerably, occasionally to the point that the lake dries out in summer. Water chemistry is of the type $Na^+$-$Mg^{2+}$-$Cl^-$-($SO_4^{2-}$), with important annual changes in salinity, inversely related to water volume (Comín et al. 1990). The main water input to the lake is important groundwater inflow from several aquifers that makes detritic supplies to be scarce (Sánchez et al. 2001). This underground flow across saline and

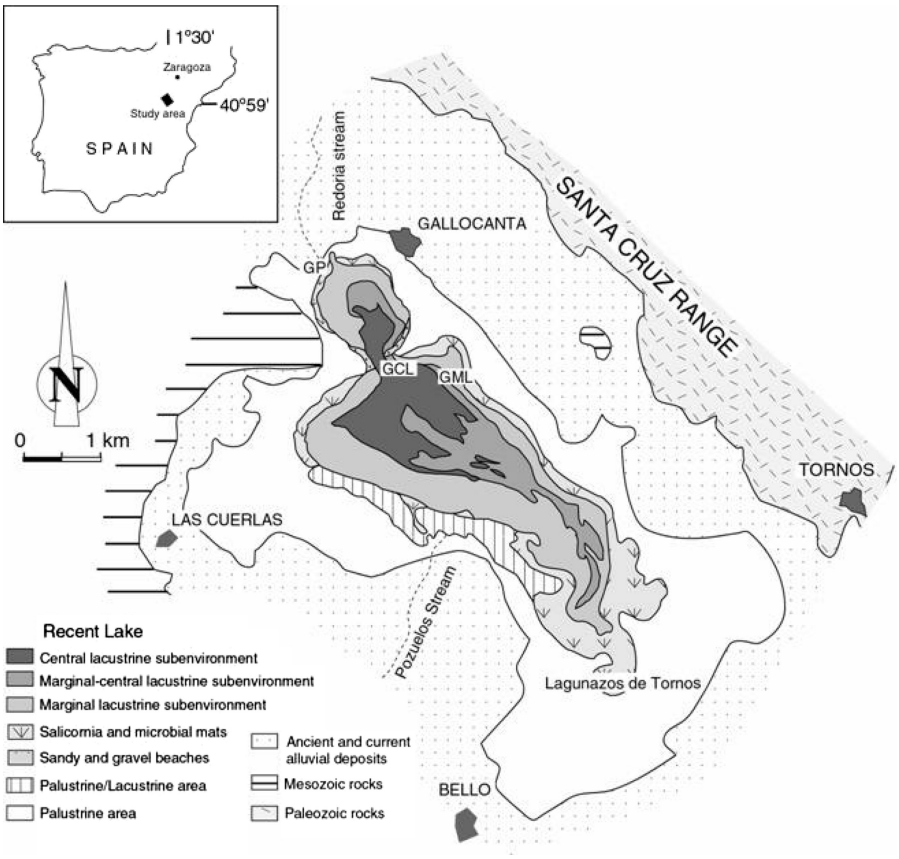


FIG. 1. Geographical location of the Gallocanta Basin and its geological setting. Facies map shows the main sedimentary subenvironments differentiated in the modern lake.

calcareous Mesozoic geological formations is the main source of sulfate for the lake water. More diluted waters from rainfall and some torrential flows reach the lake as well. The outflow is mainly by evaporation.

At the present time, carbonates predominantly form during the annual flooded periods whereas salts precipitate during dry periods. Five stratigraphic units were found in the Holocene sedimentary filling of the basin (Pérez et al. 2002). The upper and present stage corresponds to a ephemeral carbonate-rich saline lake with a high degree of organic matter preservation. This stage reflects generally lower lake levels and higher brine concentration, most likely caused by a more negative water balance. Three main depositional subenvironments can be identified in the modern lake (Pérez et al. 2002): the central lacustrine area, the marginal lacustrine area, and the palustrine area (Figure 1). Transition from central to marginal zones can be very gradual. The central lacustrine subenvironment is located in the most internal area of the lake. It is commonly flooded, even during the episodes of intense evaporation. The marginal lacustrine subenvironment occupies the major part of the lake and in the low water level episodes it can be partially or completely emerged. In the most external areas microbial mats can be recognised. The palustrine areas are developed in the NW and SE marginal zones of the lake. These zones are colonised by root vegetation and receive the inflow of some intermittent streams. Due to the extreme flat topography of the lake, they are subjected to episodic or periodic fluctuations in the water level (Figure 1). Dolomite has been found in the central lacustrine area but is absent in the most external areas of the lake where detrital input is significant and siliciclastic material more abundant (Mayayo et al. 2003). Lateral distribution of the Ca-Mg bearing carbonates in the modern sediments, indicate a direct relation of dolomite to the central area in dry periods. A detrital origin of the Ca-Mg carbonates in this lake seems very unlikely.

## MATERIALS AND METHODS

### Sampling and Water Chemistry

Samples for microbiological, microecological, and mineralogical studies were collected from the three sedimentary subenvironments recognised in the modern Gallocanta Lake: central lacustrine (GCL), marginal lacustrine (GML) and palustrine (GP). Water conductivity (Jenway conductivity meter) and pH (Crison pH-meter) were measured at each site, and water samples were collected for chemical analyses. Sulfate concentration and total alkalinity were determined according to Rodier (1984), and magnesium and calcium by atomic absortion spectrophotometry (APHA 1989). Saturation index (SI)

for dolomite, calcite and aragonite were calculated from water chemistry data using the software PHREEQC (Parkhurst 1995) and the mean water temperature for April (12.5°C).

## Microelectrode Measurements

Microelectrodes provide the possibility of measuring steep chemical gradients at fine spatial resolution and with a minimum disturbance. Vertical profiles of $O_2$, $H_2S$, pH, and Eh at the water-sediment interface were measured with microelectrodes (Unisense, Denmark) in sediment cores collected from each site. Samples of the upper 5 cm of sediment were collected with plexiglass cores (54 mm internal diameter), which were sealed and transported in the dark at 4°C to the laboratory. The sediment cores from each site were kept at 20°C in a 10 h light: 14 h dark photoperiod for 5 to 8 days in a flow chamber with a temperature-controlled continuous water flow (Lorenzen et al. 1995; García de Lomas et al. 2005). Irradiance during the light period was 200–350 $\mu$mol $m^{-2}$ $s^{-1}$ (LiCor, plane sensor). The liquid medium was diluted seawater, or seawater supplemented with NaCl, $MgSO_4$, and $CaCl_2$ to obtain salinities identical to those measured in the field for every site: 5 (GP), 25 (GML), and 116‰ (GCL), respectively. We decided to mimic the Gallocanta natural water of each subenvironment as described above because it was impossible to transport the large volume of water needed for microelectrode measurements under continuous water flow.

Dissolved oxygen was measured by a Clark-type oxygen microelectrode with a guard cathode (Revsbech 1989; García de Lomas et al. 2005) connected to a picoammeter with the polarization voltage set at–800 mV (PA-2000, Unisense). The microelectrode had a tip diameter of 25 $\mu$m, 90% response time of 0.4 s, and a stirring sensitivity of 1%. A two-point calibration of the microelectrode was done from its reading in the air-saturated bulk water above the sediment surface (100% $O_2$) and in the anoxic zone of the sediment (0% $O_2$). Dissolved sulfide was measured with a $H_2S$ microelectrode (Kühl et al. 1998; García de Lomas et al. 2005). This microelectrode is a miniaturized amperometric sensor with a guard electrode. The microelectrode used in our experiments had a tip diameter of 25 $\mu$m, a 90% response time between 1 to 10 s, and a stirring sensitivity lower than 2%. The microelectrode was connected to a picoammeter with the polarization voltage set at +85 mV. Calibration of the $H_2S$ microelectrode was done by adding known volumes of an anoxic 50 mM $Na_2S$ stock solution in 0.1 M NaOH to a 100 mM phosphate buffer at pH 7 in anoxic conditions ($N_2$-flushed). Sulfide concentration was calculated as follows:

$$[H_2S] = \left[S^{2-}_{tot}\right] / (1 + (K_1K_2/[H_3O^+]^2) + (K_1/[H_3O^+])) \quad [1]$$

where $[S^{2-}_{tot}]$ is the total sulfide concentration, $H_3O^+$ is the hydrogen ion activity, calculated from measured pH values. $K_1$ and $K_2$ are the first and second dissociation constants, respectively, of the sulfide equilibrium system: $pK_1 = 7.05$ and $pK_2 = 17.1$ (Kühl and Jørgensen 1992).

The pH microelectrodes needed an external reference electrode that was positioned in the bulk water during experiments and were similar to those described by Revsbech et al. (1983). The microelectrodes had a tip diameter of 25 $\mu$m and a typical response time of less than 20 s. Calibration was performed in 3 phosphate buffer solutions of known pH, covering the range of expected pH in the samples. Typically the electrodes responded with voltage changes of 50–61 mV per pH unit (García de Lomas et al. 2005). Microelectrodes for measuring redox potential, Eh, were similar to those described by Revsbech and Jørgensen (1986). The microelectrodes had a tip diameter of 25 $\mu$m and a 90% response time of less than 10 s. Calibration was done in two saturated quinhydrone solutions at pH 4 and 7, where the microelectrode displayed a voltage difference of 170–185 mV. The pH and Eh microelectrodes were connected via a high impedance mV-meter (MeterLab) to an external reference electrode positioned in the bulk water during the experiments. The signals of the picoammeter and the mV-meter were registered by a strip chart recorder. All calibrations of the microsensors were performed at the appropriate temperature and salinity. Microelectrodes were mounted on a mechanical micromanipulator (Unisense) and were driven down into the sediment with a step resolution of 100 $\mu$m. Microelectrode positioning in the sediment was observed with a binocular.

From the obtained oxygen profiles, oxygen fluxes across the sediment-water interface were calculated using the equation of Fick's first law of diffusion:

$$J_o = -D_o[dC(z)/dz], \quad [2]$$

where $D_o$ is the free solution molecular diffusion coefficient of oxygen (values were taken from tables compiled by Ramsing and Gundersen (Unisense) and [dC(z)/dz] is the linear oxygen concentration gradient in the diffusive boundary layer above the sediment surface. A negative flux indicates a net export of oxygen out of the sediment and represents the net areal photosynthesis of the microbial community present; a positive flux indicates a net uptake of oxygen and represents the areal respiration.

After the microelectrode measurements, the sediment cores were taken out of the flow chamber and samples were taken from the surface of the sediment for the analyses of chlorophyll *a*, for the examination of the biological community by light microscopy, and for mineralogical analyses.

## Pigment Determination and Optical Microscopy

Samples for chlorophyll *a* were stored at −20°C until analysis and samples for light microscopy were fixed with 3% formaldehyde diluted in the same water as used for the microelectrode measurements. Liposoluble photosynthetic pigments were extracted in 100% methanol, and chlorophyll *a* and bacteriochlorophyll *a* were both determined spectrophotometrically (Pierson et al. 1987). Chlorophyll *a* and phaeophytin *a* were measured spectrophotometrically in N,N-dimethylformamide (DMF) extracts as well (Porra et al. 1989).

## Mineralogical Analysis

Samples of the upper millimetres of sediment were dried, powdered, and analysed by X-ray diffraction (XRD) using

a Philips PW1710 diffractometer, $CuK_{\alpha}$ radiation, graphite monochromator, and automatic slit. A second analysis of samples, once washed with distilled water to eliminate the soluble phases, was done for a better determination of the proportions among the different types of carbonates. The molar percentage of $MgCO_3$ in dolomite and calcite was determined by XRD, measuring the relative position of the (104) and (101) reflections of carbonates and quartz, respectively, the latter being taken as standard (Goldsmith and Graf 1958; Lumsden 1979). The scanning electron microscopic study was carried out on a using JEOL JSM 6400 and ESEM FEI-Quanta 200 microscopes, coupled with an energy dispersive X-ray (EDAX) for elemental identification. Samples were carbon-coated using a sputting coater to avoid peak overlapping. SEM observations were made both in conventional SEM mode and low vacuum mode to avoid charge and collapse of organic structures.

## RESULTS

### Water Chemistry and Sediment Mineralogy

At the time of sampling, late spring, there were considerable differences in the physico-chemical properties of the water column overlaying the sediments of the three subenvironments distinguished in Gallocanta Lake (Table 1). Salinity ranged from 5‰ to 116‰ in GP and GCL subenvironments, respectively, with intermediate value (25‰) in the GML subenvironment. Associated with the salinity differences among sites there were important differences in sulfate concentration ranging from 0.156 to 18.428 g $L^{-1}$in the GP and GCL subenvironments respectively. Both $Mg^{2+}$ and $Ca^{2+}$ increased with sulfate and salinity as well. Total alkalinity did not covariate with salinity, the highest level was found in the GP site (7.38 meq $L^{-1}$) and the lowest one in the GML subenvironment (1.56 meq $L^{-1}$). The differences in pH among subenvironments were lower than 0.9 units, following a pattern inverse to salinity. Calculation of saturation index of dolomite, calcite and aragonite for every environment show that dolomite was oversaturated in all cases. Calcite and aragonite were oversaturated only in the GP subenevironment (Table 1).

TABLE 1
Some physico-chemical characteristics of the water column overlaying the sediments at the three sampled sites

| | GCL | GML | GP |
|---|---|---|---|
| Salinity (%) | 116 | 25 | 5 |
| pH | 7.80 | 7.98 | 8.66 |
| Alkalinity (meq $L^{-1}$) | 4.99 | 1.56 | 7.38 |
| $SO_4^{-2}$ (g $L^{-1}$) | 18.428 | 5.144 | 0.156 |
| $Mg^{2+}$ (g $L^{-1}$) | 7.590 | 2.118 | 0.048 |
| $Ca^{2+}$ (g $L^{-1}$) | 1.759 | 0.489 | 0.108 |
| Mg:Ca (molar ratio) | 7.12 | 7.13 | 0.73 |
| $SI_{Cc}$ | 0.89 | 0.33 | 1.53 |
| $SI_{Ar}$ | 0.73 | 0.17 | 1.38 |
| $SI_{Dol}$ | 2.62 | 1.48 | 2.89 |

Central lacustrine subenvironment (GCL), marginal lacustrine subenvironment (GML) and palustrine subenvironment (GP). Saturation index were calculated for calcite ($SI_{Cc}$), aragonite ($SI_{Ar}$), and dolomite ($SI_{Dol}$).

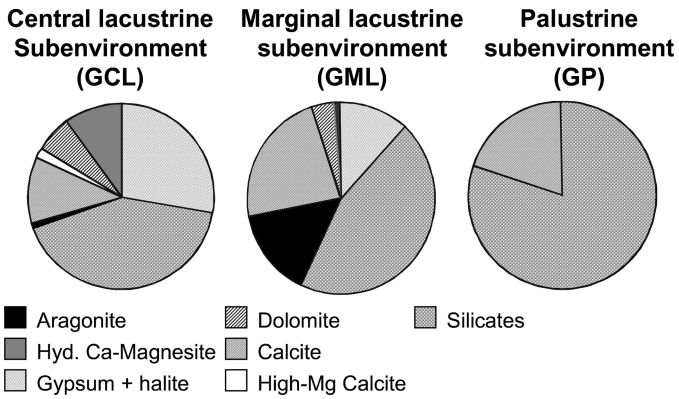


FIG. 2. Mineralogy of the upper sediment layer for the three subenvironments of Gallocanta Lake. Silicates = quartz + feldspars + phyllosilicates.

The analysis by XRD revealed important differences among the GCL, GML, and GP subenvironments (Figures 2 and 3). Ca-Mg bearing carbonates were detected in the GCL and GML subenvironments, but were more abundant in the GCL subenvironment. They were absent in the GP subenvironment where all carbonate in the upper sediment layer was calcite. Contents of sulphate and chloride minerals, gypsum and halite, followed a pattern similar to that of the Ca-Mg carbonates: they were highest in the GCL subenvironment, present in GML, and absent from the GP subenvironment. Abundance of silicates as quartz, feldspars and phyllosilicates, was the highest in the GP subenvironment and the lowest at the GCL site. Abundance of silicates can be interpreted as an indication of the relative importance of detrital material in the three sedimentary subenvironments discriminated in Gallocanta Lake.

A closer examination of the carbonate minerals revealed important differences among subenvironments as well. Carbonate minerals with different proportions of Ca and Mg were most abundant in the GCL subenvironment, followed by calcite and a very little amount of aragonite (Table 2). Among the Ca-Mg carbonates, hydrated Ca-magnesite was the dominant form (>40%

TABLE 2
Mean abundance of carbonate minerals expressed as % of total carbonate in upper 3 mm of sediment from GCL, GML, and GP subenvironments

| | Aragonite | Calcite | High-Mg Calcite | Hydrated Ca-Magnesite | Dolomite |
|---|---|---|---|---|---|
| GCL | <5 | 35 (5) | 5 (7) | 41 (7) | 15 (1) |
| GML | 35 (22) | 51 (21) | 0 | < 5 (6) | 9 (4) |
| GP | 0 | 100 (0) | 0 | 0 | 0 |

Data are the mean of 3 replicates with standard deviation within brackets.

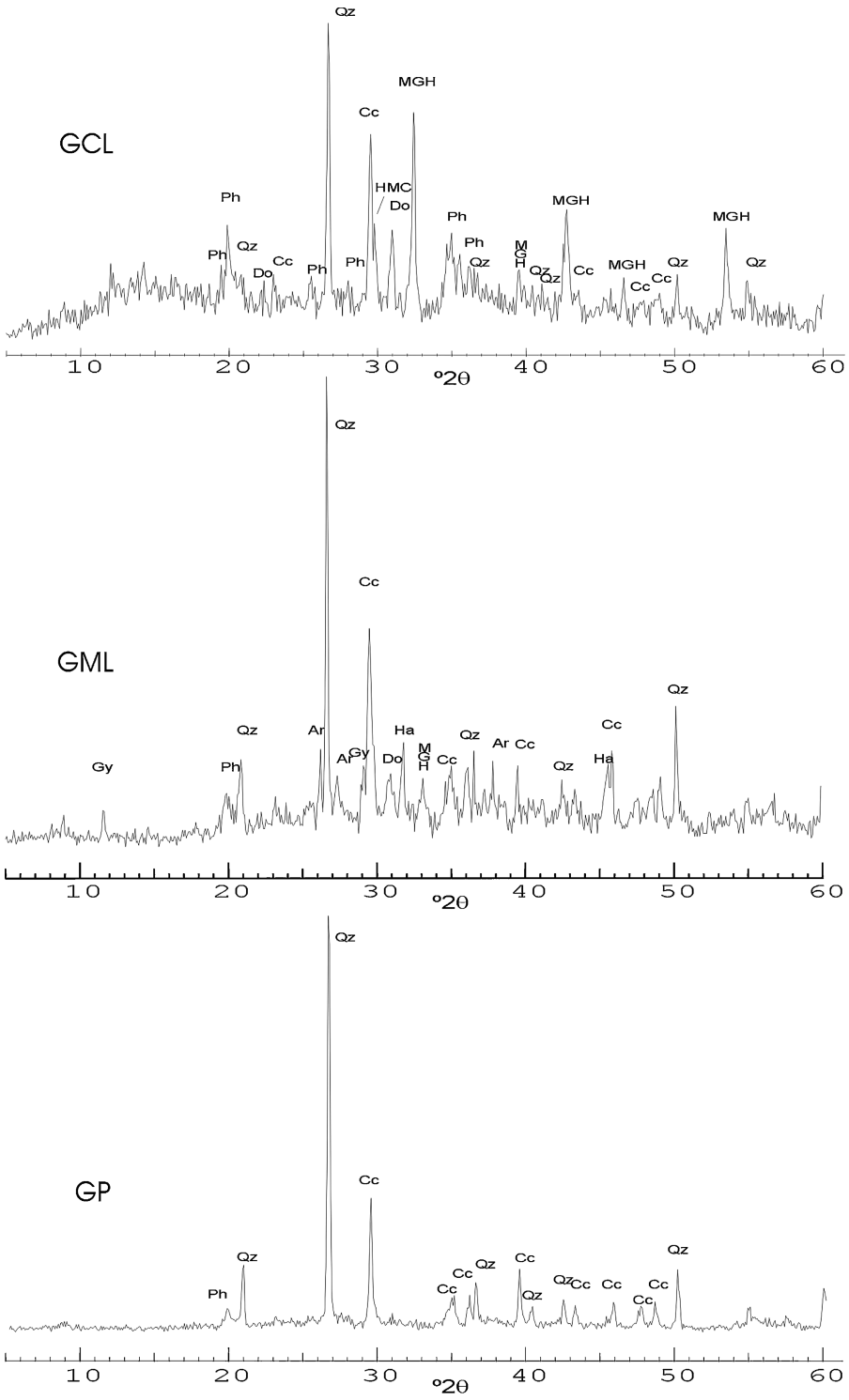


FIG. 3. X-ray diffractograms at 3-mm depth. Ph: phyllosilicates, Qz: quartz, Do: dolomite, Cc: calcite, HMC: high Mg-calcite, MGH: hydrous Ca-magnesite.

of total carbonates), followed by dolomite (15%) and a little amount of high-Mg calcite. The X-ray diffractograms show that dolomite presented a sharp reflection in $30.98^{\circ}2\theta$, suggesting a $MgCO_3$ molar % of 51% (Figure 3). Therefore the dolomite in the upper layers of the sediment in Gallocanta Lake can be considered stoichiometric and ordered. Carbonate mineralogy in the GML subenvironment was very different. Calcium carbonates like aragonite and calcite were the most abundant, $35 \pm 22\%$ and $51 \pm 22\%$ respectively, while Mg-containing carbonates were very scarce. High-Mg calcite was not detected

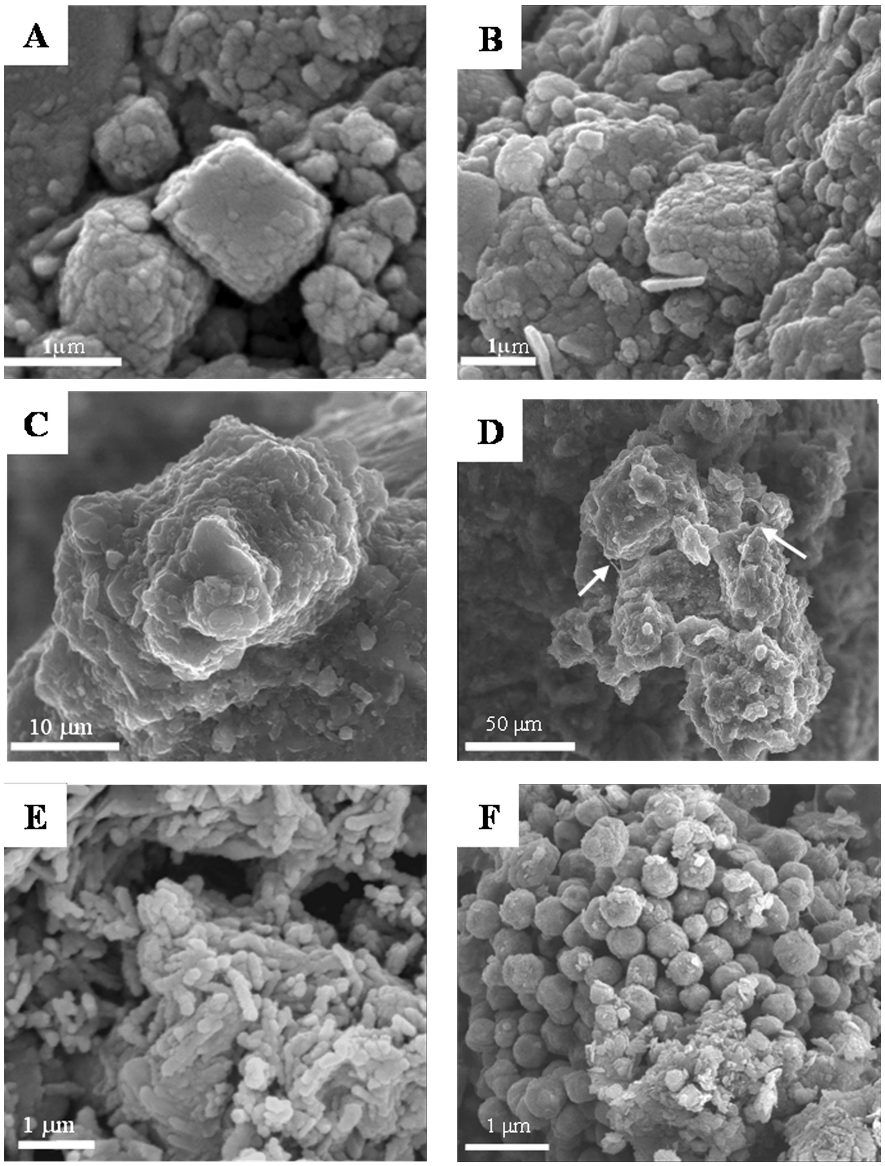


FIG. 4. Scanning electron micrographs from GCL subenvironment. (A–B) SEM images of rhombohedral Ca-Mg carbonates crystals showing knobbly surfaces. (C–D) ESEM images of carbonate crystals showing aggregates of smaller crystals and filaments (white arrows). (E) Cell-shaped morphologies on a carbonate crystal. (F) Framboid of pyrite.

at all, and dolomite was slightly less abundant. However, the major difference with the GCL subenvironment was the presence of a much smaller fraction of hydrated Ca-magnesite. In the GP subenvironment the only carbonate mineral present was calcite with a very low Mg content.

SEM observations of fragments of bulk samples showed a variety of shapes and sizes in the Ca-Mg carbonate crystals (Figure 4). Rhombohedral carbonates up to 2 $\mu$m can be observed in Figure 4A. Knobbly surface textures on Ca-Mg carbonate crystals were clearly identified in GCL samples resembling poorly crystallized dolomites as described by Vasconcelos and McKenzie (1997) in Lagoa Vermelha (Figures 4A, 4B). A few dumbbell crystal morphologies were also observed in $<3$ $\mu$m sized crystals. Bigger crystals (up to 50 $\mu$m) were also observable (Figures 4C, 4D). A detailed observation show that many of these crystals were made of aggregates of smaller individual microcrystals showing triangular shapes (Figure 4C, center of the image). Unidentified filaments (Figure 4D, arrows), 1 $\mu$m long, and cell-shaped morphologies on the surface of carbonates were also frequent (Figure 4E). Probable extracellular organic material embedding carbonate grains were common. Iron sulfides were present as framboidal aggregates showing $<1$ $\mu$m pyrite crystals (Figure 4F).

## Oxygen Profiles and Net Microbial Community Metabolism

Oxygen concentration profiles at the water-sediment interface of the GCL subenvironment were identical in light and in

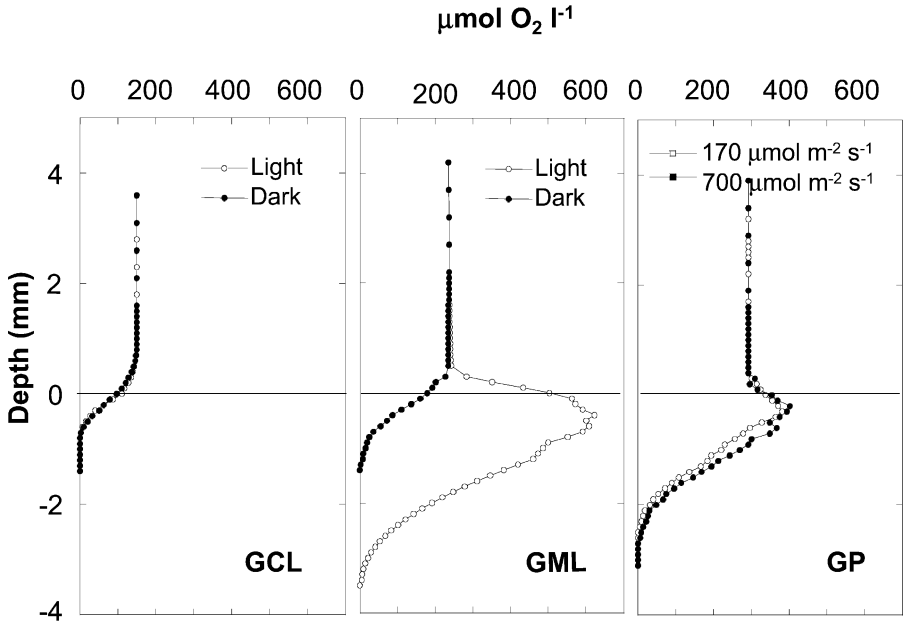


FIG. 5. Oxygen profiles at water-sediment interface in the GCL, GML, and GP subenvironments. The profiles were obtained in light and darkness for the GCL and GML subenvironments and only in light for the GP subenvironment. Light profiles were determined at a photon fluence density of 170 $\mu$mol $m^{-2}$ $s^{-1}$ for all subenvironments and also at 700 $\mu$mol $m^{-2}$ $s^{-1}$ for the GP subenvironment.

the dark (Figure 5). Therefore the microbial community in this subenvironment was not photosynthetically active, being entirely heterotrophic, or its oxygenic photosynthetic activity was below the detection level (0.3 $\mu$mol $O_2$ $L^{-1}$). The $O_2$ consumption by the sediment was similar in dark and light (0.036 nmol $O_2$ $cm^{-2}$ $s^{-1}$), and oxygen penetration in the sediment reached only 700 $\mu$m; below this depth anoxic conditions prevailed.

On the contrary, the microbial community in GML subenvironment was photosynthetically active as indicated by the differences between the $O_2$ profiles in light and dark (Figure 5). In the dark, oxygen was consumed in the sediment in the upper 1000 $\mu$m at a rate of 0.040 nmol $O_2$ $cm^{-2}$ $s^{-1}$. In light, the photosynthetic activity at the sediment surface increased the $O_2$ concentration in the upper layer of sediment, creating a net flux of $O_2$ from the sediment to the overlaying water (0.072 nmol $O_2$ $cm^{-2}$ $s^{-1}$). In addition, photosynthetic activity increased the depth of oxic layer to about 3.5 mm.

The microbial community from the GP subenvironment was also photosynthetically active as shown by its typical $O_2$ profile in light (Figure 5). Net photosynthesis rate (0.0215 nmol $O_2$ $cm^{-2}$ $s^{-1}$) was lower than for the GML subenvironment, and it was saturated at a relatively low photon fluence rate (170 $\mu$mol $m^{-2}$ $s^{-1}$) since there was almost no difference in the $O_2$ profile when measured at a much higher photon fluence rate (700 $\mu$mol $m^{-2}$ $s^{-1}$).

## Microbial Communities in the Sediment

Characterization of the microbial communities in the surface sediment of Gallocanta Lake was performed by pigment determination and optical microscopy. Photoautrophic biomass, estimated by the concentration of chlorophyll *a* (Chl *a*) and bacteriochlorophyll *a*, differed considerably among the three subenvironments. The highest concentration (100 $\mu$g Chl *a* $cm^{-2}$) was found in the GML subenvironment in accordance with the higher net photosynthesis rate observed in this environment. A much lower Chl *a* concentration (8.7 $\mu$g Chl *a* $cm^{-2}$) was found in the GP subenvironment, where oxygenic photosynthetic activity was also detected. Surprisingly, Chl *a* was detected in the GCL subenvironment as well (5 $\mu$g Chl *a* $cm^{-2}$), where no oxygenic photosynthetic activity was observed. However, a new extraction in 100% DMF allowed us to quantify the proportion of phaeopigments in this sample, which was higher than 60%. This suggests that most of the Chl *a* measured in the GCL subenvironment was detritic. The absorbance spectra of pigments extracted with methanol revealed important changes in the relative importance of different groups of photosynthetic microorganisms among subenvironments. We found an absorbance peak at 754 nm in the GCL and GP subenvironments, although less pronounced in GP. This peak probably corresponds to bacteriophaeophytin *a*, a degradation product of bacteriochlorophyll *a*. This pigment was not detected in the GML subenvironment (Figure 6).

Examination by optical microscopy of samples from the three subenvironments confirmed the absence of oxygenic phototrophic microorganisms in the GCL subenvironment. The sediment surface in the GML subenvironment was colonised by some unicellular cyanobacteria like *Merismopedia* sp. and abundant trichomes of filamentous cyanobacteria like *Oscillatoria* sp., *Lyngbya* sp. and bundles of *Microcoleus chthonoplastes*. This photosynthetic cyanobacterial community grew on the sediment surface but also colonised a layer of organic detritic

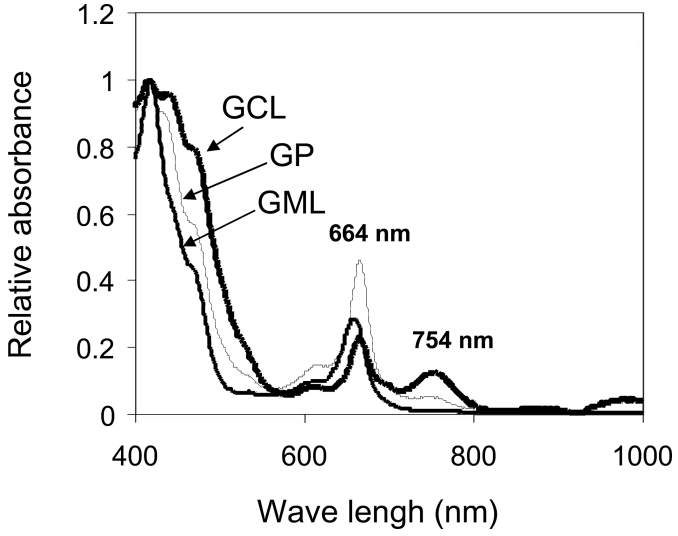


FIG. 6. Normalised absorbance spectra for extracted photosynthetic pigments from Gallocanta Lake subenvironments. Peaks at 664 and 754 nm correspond to Chl *a* and bacteriophaeophytin *a*, respectively.

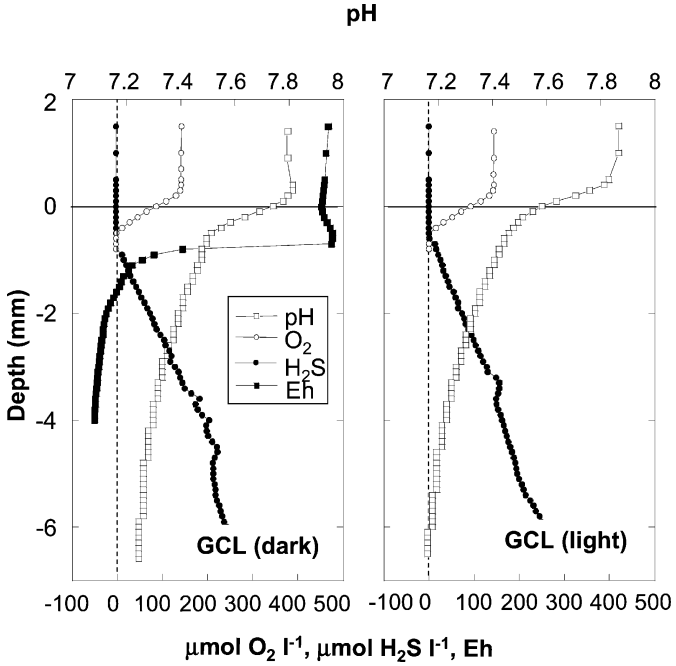


FIG. 7. Oxygen, $H_2S$, and pH profiles at the water-sediment interface in the GCL subenvironment in light and darkness. Redox potential (Eh) was measured only in darkness.

material, from macroalgae and macrophytes, that accumulates on the sediment surface in this subenvironment during the dry season. The photosynthetic community in the GP subenvironment was dominated by diatoms as *Navicula* sp. and *Nitzschia* sp. Some short trichomes of *Oscillatoria* sp. were present as well, and heterotrophic flagellates were relatively abundant.

## Chemical Microenvironment in the Sediment Surface

Since dolomite and other Mg-bearing carbonates were only found in the GCL and the GML subenvironments, to better characterise the chemical microenvironment where precipitation of Mg-bearing carbonates is taking place, a second set of experiments were done with new cores from these subenvironments. In this case, in addition to $O_2$, we measured $H_2S$, pH, and Eh in the light and in the dark.

Oxygen profiles at the water-sediment interface confirmed previous results. The benthic microbial community in the GCL site was not photosynthetically active (Figure 7). Oxygen was exhausted at about 500 $\mu$m below the sediment surface and clearly determined the strong gradient in the redox potential at this depth (Figure 7). In the GML subenvironment, the shape of the $O_2$ profiles, the depth of the oxic layer and the direction of the net flux of $O_2$ were clearly determined by the presence or absence of light, as previously shown (Figure 8).

Below the oxic layer, the mineralization of organic matter occurs by the synergic collaboration of different functional groups of anaerobic microorganisms. Dissimilatory sulfate reduction by sulfate-reducing bacteria (SRB) plays a major role when sulfate is abundant. SRB oxidise low molecular weight organic compounds with $SO_4^{2-}$ as the terminal electron acceptor and the release of $H_2S$ to the external medium. By means of $H_2S$ microelectrodes we could measure this compound in cores from the GCL and GML subenvironments at a high resolution without disturbing the sediment vertical structure. Our results show important differences in the concentration of $H_2S$ among the sediments of the GCL and the GML subenvironments (Figures 7 and 8).

In the GCL subenvironment, sulfide was absent from the water column and from the sediment oxic layer, but it was present

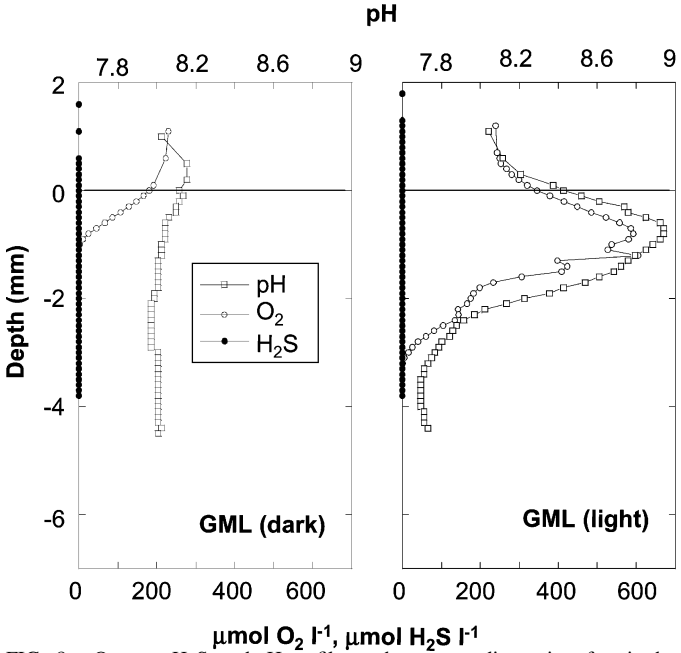


FIG. 8. Oxygen, $H_2S$, and pH profiles at the water-sediment interface in the GML subenvironment in light and darkness.

below the oxic layer and increased with depth. The maximum depth reached in this experiment was 6–7 mm below the sediment surface and the $H_2S$ concentration at this depth was higher than 250 $\mu$mol $H_2S$ $L^{-1}$. The $S_2^-/HS^-/H_2S$ equilibrium is pH dependent; equation [1] and the measured pH changes within the sediment allow us to calculate that the percentage of $H_2S$ to total sulfide ($[S^{2-}_{tot}]$) increased steadily with depth from 21% at the bottom of the oxic layer to 30% at 6 mm depth. As expected there were no differences between the $H_2S$ vertical profiles in the dark and in light (Figure 7). In the sediment cores from the GML subenvironment we did not detect $H_2S$ in the upper 6 mm of sediment, despite the fact that in the dark the oxic layer was restricted to the upper 1 mm (Figure 8).

The pH at the water-sediment interface was strongly affected by photosynthetic activity in the GML subenvironment (Figure 8). In light, the shape of the pH vertical profile was similar to that of the $O_2$ profile. A maximum pH close to 9 was observed at 1 mm below the sediment surface, coincident with a maximum in $O_2$ concentration. In contrast, in the dark, the pH of interstitial water hardly changed with depth and remained close to the pH of bulk water near 8. The vertical profiles of pH in the GCL subenvironment were, as expected, similar in the dark and light. We detected important pH changes in the upper layer of sediment, from 7.8 in the water column to 7.2 at 6 mm below the sediment surface in both cases (Figure 7).

## DISCUSSION

### Water Chemistry and Sedimentary Subenvironments

Previous studies, based on stratigraphic and facies analysis, showed the existence of three sedimentary subenvironments in Gallocanta lake: central lacustrine, marginal lacustrine, and palustrine (Pérez et al. 2002). Our results show also important differences in water chemistry, mineralogical composition, and biological community and activities among the three subenvironments. Particularly relevant for the speciation of carbonate precipitation are the differences in salinity and $SO_4^{2-}$ concentration in the water column (Table 1). The GP, GML, and GCL subenvironments represent different stages in a gradient of increasing salinity and $SO_4^{2-}$ concentration.

In late spring, salinity ranged from 5‰ in GP to 116‰ in the GCL subenvironment, and associated with it there were important differences in the $SO_4^{2-}$ concentration, from 0.156 to 18.43 g $L^{-1}$, respectively. For comparison, seawater contains ca. 2.7 g $SO_4^{2-}$ $L^{-1}$. $Mg^{2+}$ and $Ca^{2+}$ concentrations were closely related with changes in salinity and sulfate, contributing further to the differences in water chemistry between subenvironments. Through the annual hydrological cycle, in the Gallocanta Lake, increases in salinity are highly correlated with increases in $Na^+$, $K^+$, and $Mg^{2+}$, and with $Cl^-$ and $SO_4^{2-}$ concentrations (Comín et al. 1990). Therefore, salinity and sulfate changes are good tracers of $Mg^{2+}$ concentration in the water column in this lake. On the contrary, $Ca^{2+}$ concentration increased with salinity from April to August and decreased with salinity due to intense precipitation from August to October (Comín et al. 1990).

Necessarily, the precipitation of Mg-bearing carbonates only occurs when the Mg/Ca ratio is high enough. However the Mg/Ca ratio is not the only controlling factor for dolomite formation because this mineral and other Mg-bearing carbonates precipitate in environments with very different Mg/Ca stoichiometries. Organogenic dolomite precipitation occurs in marine sediments at Mg/Ca ratios between 5 and 16 (Middelburg et al. 1990). Mg/Ca was as low as 4.1 in the superficial water of Lagoa Vermelha in the dry season, when dolomite precipitation occurs (Vasconcelos and McKenzie 1997), and it ranged from 13.2 to 52.8 in the ephemeral distal lakes of the Coorong region (Wright 1999). Finally, Vasconcelos et al. (1995) precipitated dolomite in the laboratory in the presence of SRB at Mg/Ca ratio close to 16 (molar ratio). The spatial heterogeneity in the water column of Gallocanta Lake regarding the Mg/Ca ratio was considerable, from 0.7 in the GP subenvironment to more than 7 in the GML and GCL subenvironments. Differences even larger were found in the interstitial water, from 1.5 at the shore to 40 in the central part, being this variability mainly due to differences in the $Mg^{2+}$ concentration (Comín et al. 1990).

The mineralogical composition of the upper sediment layer changed with differences in water chemistry among subenvironments (Table 2). The highest abundances of high-Mg calcite, hydrated Ca-magnesite and dolomite were found in the GCL subenvironment, where $Mg^{2+}$ concentration was the highest. The absolute Mg concentration seems to be more important than the Mg/Ca ratio because there were large differences in the abundance of Mg-bearing carbonates between GCL and GML subenvironments for similar Mg/Ca ratios. No Mg-bearing carbonates were found in the GP subenvironment, where both $Mg^{2+}$ and Mg/Ca ratio were the lowest. However, SI calculations based in the water chemistry of late spring indicate that dolomite must precipitate in the GP subenvironment. Maximum abundances of dolomite were found in the GCL subenvironment, with lower SI but high sulfate-reduction activity in the sediments. Despite of being slightly oversaturated, no aragonite was found in the GP subenvironment (Table 1).

The source of sulfate ions in Gallocanta Lake is mainly the groundwater inflow across saline and calcareous formations and consequent concentration in this evaporitic endorheic basin. This is a major difference with other geological settings, where primary dolomite precipitation occurs at present. In the majority of cases the source of sulfate is sea water. In anoxic marine sediments sulfate diffuses from the water column into the sediment where it is exhausted by SRB, primary dolomite precipitation occurring below the zero sulfate level, at 1 to 10 m depth within the sediment (Compton 1988; Middelburg et al. 1990). This sulfate-free layer is unlikely to occur in Gallocanta Lake due to the importance of groundwater inflow as a source of sulfate. Similarly, it is unlikely to occur in the ephemeral lakes of the Coorong area in Australia or in Lagoa Vermelha in Brazil, where the major source of sulfate is seepage from the sea. In these two

environments, dolomite precipitation occurs in the upper layers of sediment or even within an anoxic black sludge at the sediment surface (Vasconcelos and McKenzie 1997; Wright 1999).

## Microbial Communities and Activities

The microbial communities from the three subenvironments were very different. Microbenthos of the GCL subenvironment was heterotrophic (Figures 5 and 7). The absence of oxygenic photosynthesis determines the oxygen net exchange at the water-sediment interface and the depth of the oxic layer within the sediment. On a daily basis the oxygen consumption in the oxic layer of the GCL subenvironment by biotic (mainly aerobic respiration and $H_2S$ biological oxidation) and abiotic processes (mainly chemical oxidation of $H_2S$) was 31.1 mmol $O_2$ $m^{-2}$ $d^{-1}$. This $O_2$ diffuses from the overlying water to the sediment, being a net sink for $O_2$ during both day- and night-time since there were no differences in the oxygen profiles. Below the oxic layer, organic matter is mineralised by the co-operative action of several functional groups of organisms, a complex fermenting community and SRB when sulfate concentration is high (Fenchel and Finley 1995). Under anoxic conditions, sulfate-reducing bacteria use $SO_4^{2-}$ as a terminal electron acceptor for the oxidation of organic carbon. The activity of SRB leads to a decrease in $SO_4^{2-}$ and a stoichiometric release of $H_2S$ (Figure 7), according to the following general reaction

$$2CH_2O + SO_4^{2-} \rightarrow 2HCO_3^- + H_2S \qquad [3]$$

In addition, sulfate reduction activity increases carbonate alkalinity, facilitating the precipitation of carbonates (Chafetz and Buczynski 1992; Visscher et al. 1998; Visscher et al. 2000; Dupraz et al. 2004). Depending on the stoichiometric composition of the organic matter being mineralized; sulfate reduction might produce a slight decrease of pH that could promote carbonate dissolution, however the build up of alkalinity increases the saturation state of porewater and will, ultimately, lead to the precipitation of carbonates (Jahnke et al. 1994; Mucci et al. 2000; Visscher et al. 2000).

On the contrary, in the GML subenvironment, assuming a day cycle of 12 h light:12 h dark, the sediment is a sink of $O_2$ during night time (17.3 mmol $O_2$ $m^{-2}$ $d^{-1}$) and it releases $O_2$ during the light period due to photosynthetic activity (31.1 mmol $O_2$ $m^{-2}$ $d^{-1}$). On a daily basis, the sediment of the GML subenvironment will be a net source of $O_2$ (13.8 mmol $O_2$ $m^{-2}$ $d^{-1}$) for the overlaying water. Similarly, part of the oxygen produced by the microphytobenthic community during day time diffuses down into the sediment increasing the depth of the oxic layer by up to 3.5 mm (Figures 5 and 8), and therefore enhancing aerobic biotic and abiotic processes within the sediment. Diel fluctuations in the depth of the oxic-anoxic transition zone have been shown to play a role in the precipitation and dissolution of carbonates (Visscher et al. 1998). During daytime photosynthetic activity consumed $CO_2$ and increased the pH of the upper sediment layer (Figure 8). The capacity of oxygenic photosynthetic organisms to facilitate $CaCO_3$ precipitation in a number of environments is well known, and it is explained by shifts in pH due to $H^+$ uptake during photosynthesis, thus inducing carbonate supersaturation (Thompson and Ferris 1990; Riding 2000). The aerobic oxidation of organic matter in the oxic layer decreases pH and lowers the saturation state of pore water with respect to carbonate minerals leading to carbonate dissolution (Jørgensen and Cohen 1977; Jahnke et al. 1994). Although oxygenic photosynthesis increases pH and therefore favours carbonate precipitation, the combination of oxygenic photosynthesis and aerobic respiration in microbial mats might result in little or no net precipitation of calcium carbonate when both microbial activities coincide in time and space within the mat (Visscher et al. 1998). However, surface of carbonate crystals showed knobbly and irregular textures that it would mean growing features instead of dissolution features (Figure 4).

Surprisingly, we detected $H_2S$ in the GCL subenvironment but not in the GML subenvironment (Figure 7). The absence of sulfide in the upper anoxic layer of the GML subenvironment could be due to the absence of significant sulfate reduction activity in this subenvironment. A perfect coupling between sulfate reduction rate and sulfide oxidation by biotic and abiotic processes, avoiding the accumulation of sulfide to detectable amounts within the sediment may be an alternative explanation. Sulfate limitation seems unlikely because the concentration of $SO_4^{2-}$ in the GML subenvironment was twice as high as the concentration in seawater, where $SO_4^{2-}$ is assumed never to be a limiting factor for sulfate reduction. Although photosynthetic activity in the GML subenvironment provided a source of organic carbon, it also stimulated its aerobic degradation by increasing the oxygen penetration depth. Framboidal pyrite was observed both in the GCL and in the GML subenvironments suggesting a certain rate of $H_2S$ production even in the latter case (Figure 4). The reaction of sedimentary iron oxide and hydroxide minerals with $H_2S$ to form pyrite can buffer sulfide to low levels even in the presence of relatively high rates of sulfate reduction (Pyzik and Sommer 1981; Canfield 1989, 1991). The pigment composition of both microbial communities also supported the existence of higher sulfate reduction rates in the GCL subenvironment than in the GML subenvironment. Bacteriophaeophytin *a* is a degradation product of bacteriochloropyll a, which is present in purple sulfur bacteria that use sulfide as an electron donor in anoxygenic photosynthesis. Competition between anoxygenic phototrophic bacteria and colorless sulfur bacteria for sulfide has been described in microbial mats (Visscher et al. 1992).

Sulfate reduction is apparently essential for primary dolomite precipitation in marine sediments (Compton 1988), within the black sludge in Lagoa Vermelha (Vasconcelos and McKenzie 1997), and in laboratory incubations (Vasconcelos et al. 1995). Abundance of dolomite and other Mg-bearing carbonates was the highest in the GCL subenvironment where likely a larger fraction of organic matter was being mineralised by sulfate

reduction in the presence of a high porewater Mg:Ca ratio. The small content of dolomite and hydrated Ca-magnesite in the GML subenvironment is likely explained by lower sulfate reduction activity at this site. Finally, at the GP site, where the concentration of sulfate was very low, dissimilatory nitrate reduction and methanogenesis likely replace sulfate reduction as major anaerobic pathways for the full oxidation of organic carbon (Fenchel and Finlay 1995). In this subenvironment only calcite was found (Table 2).

## An Ecophysiological Model for SRB-Facilitated Dolomite Precipitation

Our results show that in Gallocanta Lake the presence of dolomite and other Mg-containing carbonates is mainly associated with the activity of sulfate-reducing bacteria. Since the work of Nadson (1928), a number of authors have noticed the relationship between primary dolomite precipitation and habitats where sulfate reduction plays a critical role in the anaerobic oxidation of organic matter (Neher 1959; Gunatilaka 1987; Compton 1988; Middelburg et al. 1990). Isotopic analysis have demonstrated a significant contribution of carbon derived from the decomposition of organic matter in the primary precipitation of dolomite in anoxic marine sediments and in the anoxic black sludge of Lagoa Vermelha (Middelburg et al. 1990; Vasconcelos and McKenzie 1997). Finally, Vasconcelos et al. (1995) were able to precipitate dolomite in laboratory cultures inoculated with an anaerobic microbial community containing SRB from the *Desulfovibrio* group, isolated from Lagoa Vermelha (see also Warthmann et al. 2000).

The detailed mechanism of SRB-facilitated dolomite precipitation is still unknown. Warthmann et al. (2000) suggested that a single bacterial cell might serve as a nucleation point for the initial stage of crystal growth. External bacterial surfaces might concentrate cations from the surrounding water phase, due to the overall negative charge of the organic macromolecules that form their cell wall and exopolymeric matrix. Hence, they serve as nucleation centers for mineral precipitation with anions from the external medium as counter-ions (Decho 1990; Schultze-Lam et al. 1996; Fortin et al. 1997; Douglas and Beveridge 1998). Van Lith et al. (2003a) showed the specific adsorption of $Ca^{2+}$ and $Mg^{2+}$ to cell surfaces of SRB able to precipitate dolomite. At the scale of typical SRB cells (a few microns), mass transport occurs only by molecular diffusion and theirs cells are always surrounded by a diffusive boundary layer (DBL). The thickness of the DBL is similar to the characteristic length of the cell (Karp-Boss et al. 1996; Schulz and Jørgensen 2001). This "diffusion-halo" represents a chemical microenvironment surrounding the bacterial cell, where substrates, including electron acceptors, are depleted compared with their concentration in the bulk water phase.

The contrary applies to the metabolic by-products, including the reduced forms of the electron acceptors released by the bacteria, its concentration would be higher within the DBL. Likely, the major contribution of SRB to primary precipitation of Mg-containing carbonates is their ability to create the appropriate chemical microenvironment, where the concentrations of relevant ions for dolomite precipitation differ considerably from those of the bulk interstitial water phase. The schematic model presented in Figure 9 shows the way in which SRB are likely to modify the physicochemical conditions in their DBL, leading to primary precipitation of dolomite and other Mg-containing carbonates in close association with the cell. It aims to integrate the available information, taking into account the major processes which are likely to be involved in microbial-mediated precipitation of Mg-containing carbonates (Vasconcelos et al. 1995; Schultze-Lam et al. 1996; Fortin et al. 1997; Vasconcelos and McKenzie 1997; Van Lith et al. 2003a, 2003b).

In the bacterial cell, low molecular weight organic compounds obtained from the external medium [1], are oxidised to $CO_2$ [2], which is released to the DBL [3]. Electrons from the oxidation of organic compounds will be passed through a set of electron transporters, located in the cell membrane [4], to $SO_4^{2-}$, which will be reduced to $H_2S$ [5] and released to the DBL. The electron flow through the anaerobic respiratory chain is associated with $H^+$-pumping to the external medium [6]; this creates an electrochemical gradient that will favour the entry of $H^+$ across the ATP-synthase [7]. Finally, the thermodynamically favourable entry of $H^+$ in the cell is coupled to ATP synthesis in a well-constrained stoichiometry ($3H^+$: ATP) [7]. In addition, the $Ca^{2+}$ and $Mg^{2+}$ ions are adsorbed to the electronegative bacterial cell wall and/or exopolymer matrix surrounding the cell (Van Lith et al. 2003b), increasing their concentration compared to the water phase [8].

The amount of $H^+$ translocated to the external medium per electron passing the respiratory electron transport chain is a function of the redox potential difference between the electron donors (the organic substrates) and $SO_4^{2-}$ as final electron acceptor (Kröger 1999). The $H^+$ balance across the cell membrane and therefore the impact of SRB growth and activity on the external pH cannot be accurately calculated unless growth conditions, including specific substrates used (organic and inorganic), rate of growth, etc. are know. However, an increase in pH and in carbonate alkalinity is generally observed associated with the anaerobic oxidation of organic matter by sulfate reduction (Gaillard et al. 1989; Middelburg et al. 1990).

Heterotrophically growing SRB will sustain a net $H^+$ uptake from the external medium that will develop a diffusion-halo where pH is likely to be larger than in the bulk water phase, leading to carbonate supersaturation. In contrast, our results from the GCL subenvironment showed a decrease of almost 0.6 pH-units from the water column down to 6 mm below the sediment surface (Figure 7).

Similar decreases in pH were observed in the sulfide layer in microbial mats of a coastal hypersaline lagoon (García de Lomas et al. 2005). The interpretation of pH changes is generally arguable, because $H^+$ concentration in the sediment is the resulting balance between a large number of both biotic and abiotic

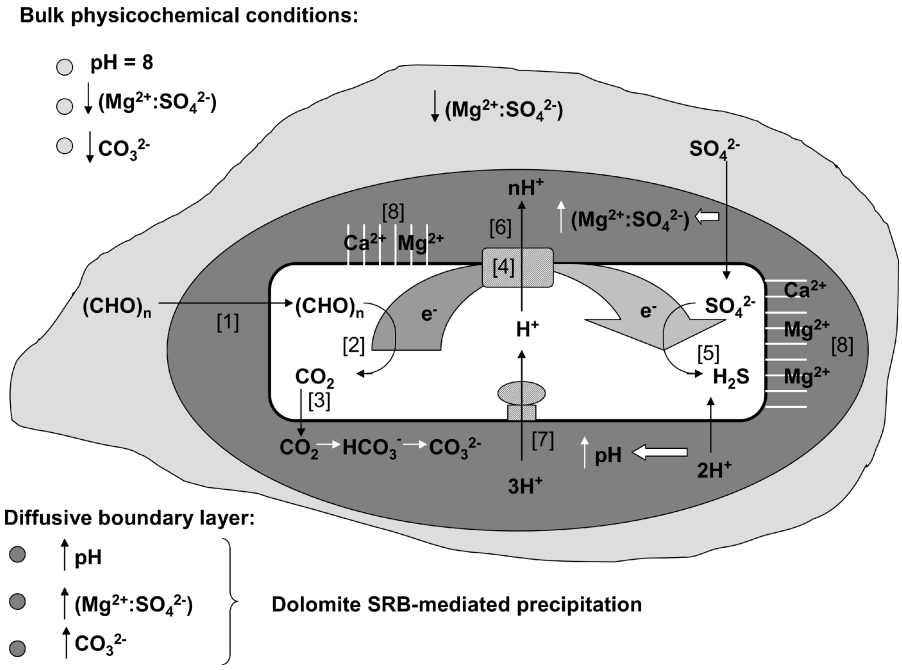


FIG. 9. Schematic model showing the major processes involved in the precipitation of Mg-bearing carbonates mediated by sulfate-reducing bacteria (SRB). The SRB cell is surrounded by a diffusive boundary layer (DBL), where the concentrations of substrates and products of the cell metabolism will be different from the bulk conditions far away from the cell. The SRB cell incorporates low molecular weight organic compounds from the external medium [1] that are oxidised to $CO_2$ [2], which is released to the DBL [3]. The electrons from the oxidation of the organic carbon pass through a set of electron transporters, located in the cell membrane [4], to $SO_4^{2-}$, which is reduced to $H_2S$ [5]. The flow of electrons across the anaerobic respiratory chain is associated with $H^+$ pumping to the external medium [6]. This creates an electrochemical gradient across the cell membrane that favours the entry of $H^+$ through the ATP-synthase, thus coupling this $H^+$ flow to the production of ATP [7]. $Ca^{2+}$ and $Mg^{2+}$ ions are adsorbed reversibly to the cell wall and the exopolymer matrix due to their net negative charge. These structures have been represented only partially for clarity [8].

processes, including dissolution and precipitation of carbonates (Visscher et al. 1998; Mucci et al. 2000). The steep decrease of pH with depth in the oxic and oxic-anoxic transition layers is probably associated with aerobic respiration and release of organic acids as end products of fermentation. Chemolitotrophic oxidation of sulfide with $O_2$ at the oxic-anoxic transition layer will also decrease pH and could contribute to carbonate dissolution (Visscher et al. 1998; Dupraz et al. 2004). Deeper in the sediment, sulfate reduction activity would damp pH changes and increases carbonate alkalinity. When the sulfate reduction layer is close to the oxic layer, $H^+$ production by the oxidation of $H_2S$ will buffer $H^+$ consumption by sulfate reduction (Jørgensen 1996). This could be the reason why we did not observe an increase in interstitial water pH in the sulfate reduction layer. The increase in carbonate alkalinity and the depletion of sulfate at the DBL of SRB cells will stimulate the precipitation of Mg-bearing carbonates if the Mg/Ca ratio is high enough. On the contrary, in the GML subenvironment, the pH profile was clearly affected by photosynthetic activity, increasing pH up to almost 9 at 1 mm depth in the light. The mineralogical data show that in this subenvironment carbonate precipitation was mainly as $CaCO_3$ in the form of calcite (51%) and aragonite (35%). The capacity of oxygenic photosynthetic organisms to facilitate $CaCO_3$ precipitation in a number of environments is well known (Thompson and Ferris 1990; Riding 2000). Why do dolomite and other Mg-containing carbonates not precipitate by the same mechanism? The likely explanation is the inhibitory presence of dissolved sulfate and the need for an appropriately high Mg:Ca ratio for dolomite precipitation.

Generally, $Ca^{2+}$, $Mg^{2+}$, and sulfate concentrations show strong positive correlations with salinity in aquatic environments (Hammer 1986). In nature, $Mg^{2+}$ concentration and Mg:Ca ratio that favour the precipitation of Mg-containing carbonates increase with the concentration of sulfate (Figure 10). Therefore, the relatively high Mg:Ca ratio needed to stimulate the dolomite precipitation tends be present in environments where the sulfate concentration is also high. However, several studies have demonstrated experimentally that the rate of dolomite formation was inversely related to sulfate concentration (Baker and Kastner 1981; Sibley et al. 1994). The unique role of SRB could be to avoid the sulfate inhibition by eliminating $SO_4^{2-}$ from the interstitial water, or at least from the DBL surrounding the bacterial cell.

Sulfate and $Mg^{2+}$ ions form a strong ionic association in aqueous solution. The formation of the ion pair reduces the concentration of dissociated free ions according to the equilibrium equation $MgSO_4(aq) \leftrightarrow Mg^{2+}(aq) + SO_4^{2-}(aq)$, and decreases the overall hydration state of $Mg^{2+}$. The equilibrium

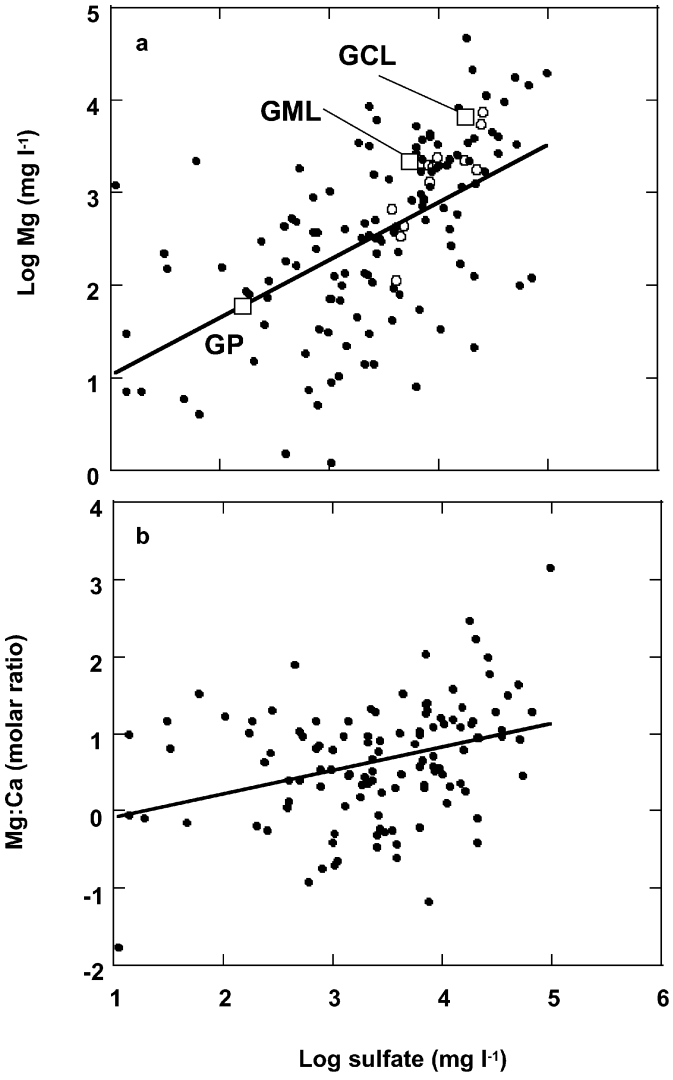


FIG. 10. Relationship between $Mg^{2+}$ and sulfate concentration (a), and Mg:Ca molar ratio and sulfate concentration (b), in 130 representative saline lakes of different salinities (black circles). Data were obtained from appendix C in Hammer (1986). In the upper plot we have also represented the covariation between $Mg^{2+}$ and sulfate for each of the subenvironments in Gallocanta Lake in spring during this study (empty squares), and for the annual cycle in GCL subenvironment (empty circles, data obtained from Comín et al. 1990). Regression equations for plots a and b: Log Mg = 0.403 + 0.623 Log sulfate ($r^2 = 0.299$, n = 130, $p < 0.01$), Log Mg:Ca = −0.615 + 0.304 Log sulfate ($r^2 = 0.100$, n = 130, $p < 0.01$).

concentration of the $MgSO_4$(aq) ion pair increases with ionic strength and therefore with salinity, however the hydration energy of $Mg^{2+}$ decreases. These two effects of salinity seem to act on dolomite precipitation in opposite directions. The decrease of free $Mg^{2+}$(aq) as a consequence of a higher degree of complexation with sulfate and $Cl^-$ as salinity increases will reduce the dolomite precipitation rate (Machel and Mountjoy 1986; Pokrovsky and Schott 2001). On the other hand, high salinity, and concomitantly sulfate concentration, may enhance the rate of dolomite formation by decreasing the hydration energy of $Mg^{2+}$ and $Ca^{2+}$ (Lippmann 1973; Machel and Mountjoy 1986; Brady et al. 1996). The genesis of other Ca-Mg bearing carbonates may follow the same process, and could also be controlled by the Mg/Ca ratio. In this study we have detected Ca-Mg hydrated magnesite in the central areas of the lake, where dolomite is more abundant. Whether hydrous Ca-magnesite is a stable phase or an intermediate step towards a more stable phase, following Ostwald step rule, is still unknown.

## CONCLUSIONS

This study shows that the three sedimentary subenvironments recognized in Gallocanta Lake, GCL, CML, and GP, represent different stages in a biogeochemical gradient. This gradient is mainly characterised by differences in salt content, which are associated with differences in the absolute and relative concentrations of sulfate, $Mg^{2+}$, $Ca^{2+}$, and the Mg:Ca ratio. Every subenvironment presented distinctly different microbiological communities and activities. The differences in water chemistry and microbiology explain the different authigenic mineralogical associations found in each of the subenvironments.

In the GCL subenvironment, the absence of oxygenic phototrophs contributes to the existence of permanent anoxic conditions very close to the sediment surface, where the input of new organic carbon from the water column occurs. Anoxic conditions and the high concentrations of sulfate favoured the role of sulfate reduction as a major biogeochemical pathway for the oxidation of organic carbon in the GCL subenvironment. The presence of SRB, with their capacity to deplete sulfate from the DBL around the cell, increasing at the same time inorganic carbon availability, and likely also pH, will induce carbonate precipitation. If previous conditions are met, the relative abundance of metal ions as counterions for carbonate precipitation could determine what type of carbonate will precipitate. Probably, the high $Mg^{2+}$ content in the pore water and a relatively high Mg:Ca ratio in the GCL subenvironment favour the formation of various Mg-bearing carbonates, including high-Mg calcite, hydrous Ca-magnesite, and dolomite. Permanently anoxic conditions are found in the GML and GP subenvironments as well. However, it is likely that a progressively lower fraction of organic carbon is being oxidized in the GML and GP subenvironments by sulfate reduction due to lower sulfate availability and to oxygenation of sediment by photosynthesis. In addition, the existence of lower Mg:Ca ratios favours the precipitation of carbonates with a lower $Mg^{2+}$ content as counterion in the GML subenvironment, and of carbonates with exclusively $Ca^{2+}$ in the GP subenvironment.

Our results show how the precipitation of different types of carbonates, particularly with different proportions of $Ca^{2+}$ and $Mg^{2+}$, occurs in the same lake along a spatial biogeochemical gradient imposed by differences in salinity. The suitable conditions for the precipitation of carbonates with different proportions of $Ca^{2+}$ and $Mg^{2+}$ might vary also seasonally. Changes along the annual cycle in salinity, sulfate and $Mg^{2+}$ concentrations, together with changes in the microbial

community are a common feature of Gallocanta Lake and similar environments.

## REFERENCES


APHA. 1989. Standard Methods for the Examination of Water and Wastewater. 17th edition. Washington DC: American Public Health Association, 1268 p.

Baker PA, Burns SJ. 1985. The occurrence and formation of dolomite in organic-rich continental margin sediments. Bull Am Assoc Petrol Geol 69:1917–1930.

Baker PA, Kastner M. 1981. Constraints on the formation of sedimentary dolomite. Science 213:214–216.

Brady PV, Krumhans JL, Papenguth HW. 1996. Surface complexation clues to dolomite growth. Geochim Cosmochim Acta 60:727–731.

Canfield DE. 1989. Reactive iron in marine sediments. Geochim Cosmochim Acta 53:619–632.

Canfield DE. 1991. Sulfate reduction in deep-sea sediments. Am J Sci 291:177–189.

Castanier S, Le Métayer-Levrel G, Perthuisot JP. 1999. Ca-carbonates precipitation and limestone genesis-the microbiologist point of view. Sediment Geol 126:9–23.

Castanier S, Le Métayer-Levrel G, Perthuisot JP. 2000. Bacterial roles in the precipitation of carbonate minerals. In Riding RE, Awramik SM, editors. Microbial Sediments. Berlin: Springer–Verlag, p. 32–39.

Chafetz HS, Buczynski C. 1992. Bacterially induced lithification of microbial mats. Palaios 7:277–293.

Chafetz HS, Imerito-Tetzlaff AA, Zhang JL. 1999. Stable isotope and elemental trends in Pleistocene sabkha dolomites: descending meteoric water vs. sulfate reduction. J Sediment Res Sect A 69 (1A):256–266.

Comín FA, Alonso M, López P, Comelles M. 1983. Limnology of Gallocanta Lake, Aragón, northeastern Spain. Hydrobiologia 105:207–221.

Comín F, Julià R, Comín P, Plana F. 1990. Hydrogeochemistry of Lake Gallocanta (Aragón, NE Spain). Hydrobiologia 197:51–66.

Compton JS. 1988. Degree of supersaturation and precipitation of organogenic dolomite. Geology 16:318–321.

Compton JS, Siever R. 1986. Diffusion and mass balance of Mg during early dolomite formation, Monterey Formation. Geochim Cosmochim Acta 50:125–135.

Decho AW 1990. Microbial exopolymer secretions in ocean environments their role(s) in food webs and marine processes. Oceanogr Mar Biol Annu Rev 28:73–153.

Douglas S, Beveridge TJ. 1998. Mineral formation by bacteria in natural microbial communities. FEMS Micro Ecol 26:79–88.

Dupraz C, Visscher PT, Baumgartner LK, Reid RP. 2004. Microbe-mineral interactions: early carbonate precipitation in a hypersaline lake (Eleuthera Island, Bahamas). Sedimentology 51:745–765.

Fairbridge RW. 1957. The dolomite question. In RJ LeBlanc, JG Breeding, editors. Regional Aspects of Carbonate Deposition. Soc Econ Paleontol. Mineral Spec Publ 5:124–178.

Fenchel T, Finlay BJ. 1995. Ecology and Evolution in Anoxic Worlds. New York: Oxford University Press.

Fortin D, Ferris FG, Beveridge TJ. 1997. Surface mediated mineral development in bacteria. In Banfield JF, Nealson KH, editors. Geomicrobiology: Interactions Between Microbes and Minerals, Reviews in Mineralogy. Washington, DC: The Mineralogical Society of America, p 161–180.

Gaillard JF, Pauwels H, Michard G. 1989. Chemical diagenesis in coastal marine sediments. Oceanol Acta 12:175–187.

García de Lomas J, Corzo A, García CM, van Bergeijk SA. 2005. Microbenthos in a hypersaline tidal lagoon: factors affecting microhabitat community structure and mass exchange at the sediment-water interface. Aquat Microb Ecol 38:53–69.

Goldsmith JR, Graf DL. 1958. Structural and compositional variations in some naturally occurring dolomites. J Geol 66:678–693.

Gunatilaka A. 1987. The dolomite problem in the light of the recent studies. Modern Geol 11:311–324.

Gunatilaka A, Saleh AA, Nassar N. 1987. Calcium-poor dolomite from the sabkhas of Kuwait. Sedimentology 34:999–1006.

Hammer UT. 1986. Saline lake ecosystems of the world. Dordrecht, The Netherlands: Dr. Junk Publishers.

Jahnke RA, Craven DB, Gaillard JF. 1994. The influence of organic matter diagenesis on $CaCO_3$ dissolution at the deep-sea floor. Geochim Cosmochimic Acta 58:2799–2809.

Jørgensen BB. 1996. Material Flux in the Sediment. In Jørgensen BB, Richardson K, editors. Eutrophication in Coastal Marine Ecosystems. Coastal and Estuarine Studies, Volume 52. Washington, DC: American Geophysical Union. p. 115–135.

Jørgensen BB, Cohen Y. 1977. Solar Lake (Sinai): 5 The sulfur cycle of the benthic cyanobacterial mat. Limnol Oceanogr 22:657–666.

Karp-Boss L, Boss E, Jumars PA. 1996. Nutrient fluxes to planktonic osmotrophs in the presence of fluid motion. In Ansell, AD, Gibson RN, Barnes MB, editors. Oceanography and Marine Biology: An Annual Review. London: UCL Press, p 71–107.

Kröger A. 1999. Electron-transport-coupled phosphorylation. In Lengeler JW, Drews G, Schlegel HG, editors. Biology of the Prokaryotes. Oxford: Blackwell Science. p 59–67.

Kühl M, Jørgensen BB. 1992. Microsensor measurements of sulfate reduction and sulfide oxidation in compact microbial communities of aerobic biofilms. Appl Environ Microbiol 58:1164–1174.

Kühl M, Steuckart C, Eickert G, Jeroschewski P. 1998. A $H_2S$ microsensor for profiling biofilms and sediments: application in an acidic lake sediment. Aquat Microb Ecol 15:201–209.

Land LS. 1998. Failure to precipitate dolomite at 25°C from dilute solution despite 1000-fold oversaturation after 32 years. Aquat Geochem 4:361–368.

Last WM. 1990. Lacustrine dolomite–an overview of modern, Holocene and Pleistocene occurrences. Earth-Sci Rev 27:221–263.

Lippmann F. 1973. Sedimentary Carbonate Minerals. New York: Springer.

Lorenzen JR, Glud RN, Ploug H, Ramsing NB. 1995. Impact of microsensor caused changes in diffusive boundary layer thickness on $O_2$ profiles and photosynthetic rates in benthic communities of microorganisms. Mar Ecol Prog Ser 119:237–241.

Lumsden DN. 1979. Discrepancy between thin section and X-ray estimates of dolomite in limestone. J Sediment Petrol 49:429–436.

Machel HG, Mountjoy EW. 1986. Chemistry and environments of dolomitization—a reappraisal. Earth-Sci Rev 23:175–222.

Mayayo MJ, Luzón A, Soria AR, Roc AC, Sánchez JA, Pérez A. 2003. Sedimentological evolution of Holocene Gallocanta lake, NE Spain. In Valero B, editor. Limnogeology in Spain: A Tribute to Kerry Kelts. Madrid: Dpto. de Publicaciones del Consejo Superior de Investigaciones Científicas (C.S.I.C). p 359–384.

McKenzie JA. 1991. The dolomite problem: an outstanding controversy. In Müller DW, McKenzie JA, Weissert H, editors. Controversies in Modern Geology: evolution of Geological Theories in Sedimentology, Earth History and Tectonics. London: Academic Press, p 37–54.

Middelburg JJ, de Lange GJ, Kreulen R. 1990. Dolomite formation in anoxic sediments of Kau Bay, Indonesia. Geology 18:399–402.

Morita RY. 1980. Calcite precipitation by marine bacteria. Geomicrobiol J 2:63–82.

Mucci A, Sundby B, Gehlen M, Arakaki T, Zhong S, Silverberg N. 2000. The fate of carbon in continental shelf sediments of eastern Canada: a case study. Deep-Sea Res 47:733–760.

Nadson GA. 1928. Beitrag zur Kenntnis der bakteriogenen Kalkablagerungen. Archiv für Hydrobiol 19:154–164.

Neher J. 1959. Bakterien in tieferliegenden Gesteinslagen. Eclogae Geol Helv 52: 619–625.

Parkhurst DL. 1995. User's guide to PHREEQC: a computer model for speciation, reaction—path, advective—transport, and inverse geochemical calculation. US Geological Survey, Water Resource Investigations Report 95-4227, 143 p.

Pérez A, Luzón A, Roc A, Soria A, Mayayo M, Sánchez JA. 2002. Sedimentary facies distribution and genesis of a recent carbonate-rich saline lake: Gallocanta lake. Iberian Chain, NE Spain. Sediment Geol 148:185–202.

Perthuisot JP. 1975. La Sebkha el Melah de Zarzis. Genèse et évolution d'un bassin salin paralique. Trav Lab Géol ENS, Paris, 9.

Pierson B, Oesterle A, Murphy GL. 1987. Pigments, light penetration, and photosynthetic activity in the multi-layered microbial mats of Great Sipewisset Salt Marsh, Massachussets. FEMS Microb Ecol 45:365–376.

Pokrovsky OS, Schott J. 2001. Kinetics and mechanisms of dolomite dissolution in neutral to alkaline solutions revisited. Am J Sci 301:597–626.

Pontoizeau P, Castanier S, Perthuisot JP. 1997. Production bactérienne de struvite ($MgNH_4PO_4$, $6H_2O$) au cours d'expériences visant à produire des carbonates hypermagnésiens. C Roy Acad Sci Paris 323(IIa):21–28.

Porra RJ, Thompson WA, Kriedemann PE. 1989. Determination of accurate extintion coefficients and simultaneous equations for assaying chlorophylls *a* and *b* extracted with four different solvents: verification of the concentration of chlorophyll standards by atomic absorption spectroscopy. Biochim Biophys Acta 975: 384–394.

Pyzik AJ, Sommer SE. 1981. Sedimentary iron monosulfides: Kinetics and mechanism of formation. Geochim Cosmochim Acta 45:687–698.

Revsbech NP. 1989. An oxygen microelectrode with a guard cathode. Limnol Oceanogr 34:472–476.

Revsbech NP, Jørgensen BB. 1986. Microelectrodes: their use in microbial ecology. Adv Microb Ecol 9:293–352.

Revsbech NP, Jørgensen BB, Blackburn TH, Cohen, Y. 1983. Microelectrodes studies of the photosyntesis and $O_2$, $H_2S$, and pH profiles of a microbial mat. Limnol Oceanogr 28:1062–1074.

Riding R. 2000. Microbial carbonates: the geological record of calcified bacterial-algal mats and biofilms. Sedimentology 47:179–214.

Rodier J. 1984. L'analyse de l'eau, eaux naturelles, eaux résiduaires, eau de mer. Paris: Dunod.

Sagemann J, Bale SJ, Parkes RJ. 1999. Controls on the formation of authigenic minerals in association with decaying organic matter: an experimental approach. Geochim Cosmochim Acta 63 (7/8):1083–1095.

Sánchez JA, Pérez A, Roc AC, Rubio JC. 2001. Fieldtrip to Aragon. In Redondo C, editor. Groundwater and Landscape Sustainable Management. Madrid: Workshop of the Complutense-Charles Universities. p 39–66.

Schulz HN, Jørgensen BB. 2001. Big bacteria. Annu Rev Microbiol 55:105–137.

Schultze-Lam S, Fortin D, Davis BS, Beveridge TJ. 1996. Mineralization of bacterial surface. Chem Geol 132:171–181.

Sibley DF, Nordeng SH, Borkowski ML. 1994. Dolomitization kinetics in hydrothermal bombs and natural settings. J Sediment Res Sect A 64:630–637.

Thompson JB, Ferris FG. 1990. Cyanobacterial precipitation of gypsum, calcite and magnesite from natural alkaline lake water. Geology 18:995–998.

Van Lith Y, Vasconcelos C, Warthmann R, Martins JCF, McKenzie JA. 2002. Bacterial sulfate reduction and salinity: two controls on dolomite precipitation in Lagoa Vermelha and Brejo do Espinho (Brazil). Hydrobiology 485:35–49.

Van Lith Y, Warthmann R, Vasconcelos C, McKenzie JA. 2003a. Microbial fossilization in carbonate sediments: a result of the bacterial surface involvement in dolomite precipitation. Sedimentology 50:237–245.

Van Lith Y, Warthmann R, Vasconcelos C, McKenzie JA. 2003b. Sulphate reducing bacteria induce low-temperature Ca-dolomite and high Mg-calcite formation. Geobiology 1:71–79.

Vasconcelos C, McKenzie JA. 1997. Microbial mediation of modern dolomite precipitation and diagenesis under anoxic conditions (Lagoa Vermelha, Rio de Janeiro, Brazil) J Sediment Res 67(3):378–390.

Vasconcelos C, McKenzie J, Bernasconi S, Gruyic D, Tien AJ. 1995. Microbial mediation as a possible mechanism for natural dolomite formation at low temperatures. Nature 377:220–222.

Visscher PT, van den Ende FP, Schaub BEM, van Gemerden H. 1992. Competition between anoxygenic bacteria and colorless sulfur bacteria in a microbial mat. FEMS Microb Ecol 101:51–58.

Visscher PT, Reid RP, Bebout BM, Hoeft SE, Macintyre IG, Thompson JA. 1998. Formation of lithified micritic laminae in modern marine stromatolites (Bahamas): The role of sulfur cycling. Am Mineral 83:1482–1491.

Visscher PT, Reid RP, Bebout BM. 2000. Microscale observations of sulfate reduction: correlation of microbial activity with lithified micritic laminae in modern marine stromatolites. Geology 28:919–922.

Warren JK. 2000. Dolomite, occurrence, evolution and economically important assocations. Earth-Sci Rev 52:1–81.

Warthmann R, Van Lith Y, Vasconcelos C, McKenzie JA, Karpoff AM. 2000. Bacterially induced dolomite precipitation in anoxic culture experiments. Geology 28:1091–1094.

Westrich J, Berner RA. 1984. The role of sedimentary organic matter in bacterial sulfate reduction: the G model tested. Limnol Oceanogr 29:236–249.

Wright DT. 1999. The role of sulphate-reducing bacteria and cyanobacteria in dolomite formation in distal ephemeral lakes of the Coorong region, South Australia. Sediment Geol 126:147–157.